ORIGINAL ARTICLE

Interaction in POSS-poly(ethylene-co-acrylic acid) nanocomposites

Nadka Tzankova Dintcheva[1], Elisabetta Morici[2], Rossella Arrigo[2] and Francesco Paolo La Mantia[1]

Use of polyhedral oligomeric silsesquioxane (POSS) in polymer-based nanocomposites is promising for the design of high-performance materials for several applications. In this study, nanocomposites based on ethylene-acrylic acid (EAA) copolymer and POSS molecules were prepared by melt mixing. In particular, partial cage POSS with different pendent organic groups was used to investigate the interaction between the –OH groups of POSS and the acrylic functionalities of the matrix. All nanocomposites were characterized by mechanical, rheological, thermal and spectroscopic analyses. In addition, PE-POSS compounds were prepared under the same processing conditions for sake of comparison. The POSS molecules affect the properties in the molten state and usually act as a plasticizer. However, this plasticizing effect should not be evident if the host polymeric matrix is able to interact with organosilicon molecules, in which case, the POSS molecules would confer an antiplasticizer effect. Therefore, all properties measured of EAA/POSS nanocomposites are the result of two contrasting phenomena, particularly the plasticizing and reinforcement effects. Moreover, the properties of these nanocomposites depend significantly on the presence of certain functionalities in the components and on possible interactions between them.
Polymer Journal (2014) 46, 160–166; doi:10.1038/pj.2013.77; published online 2 October 2013

Keywords: antiplasticizing effect; macroscopic properties; physical interactions; POSS molecules

INTRODUCTION

Polyhedral oligomeric silsesquioxanes (POSS) are an interesting class of organosilicon compounds with a tridimensional cage structure and nanometer-scale size. Each silicon atom is bonded on average to 1.5 oxygen atoms and to a hydrocarbon group $(RSiO_{1.5})_n$.[1] In recent years, the number of studies on polymeric nanocomposite-based POSS has increased because of their hybrid inorganic-organic nature, which combines the properties of ceramics and organic polymers.[2,3] Moreover, these molecules allow a high degree of flexibility: the silicon–oxygen framework can be easily functionalized with a variety of organic substituents for fully tunable solubility and reactivity.[4,5] The organic side groups on POSS span a wide range of chemistries: fluoroalkyl,[6] alkyl, phenyl,[7] alcohol, amines, vinyl,[8] carboxylic acid, sulfonic acid, PEG,[9] acrylate, methacrylate, thiols,[10] epoxides, halides, imides, silanes and silanols.[11]

The vertex groups of the cage can be tailored depending on the chemical nature of the host matrix. To improve compatibility, the polarities of the POSS molecules and polymer must strongly match.[12] Reactive vertex groups can be chosen to achieve a chemical bond between POSS molecules themselves and/or POSS and the polymer chain.[13] Many approaches are suitable to incorporate POSS into a polymeric matrix, including melt blending,[14] cross-linking copolymerization and grafting.[15] Many studies have shown that POSS

molecules improve properties such as processability,[16] thermal stability,[17] oxidative resistance[18] and antiflammability[19] of numerous amorphous or semicrystalline thermoplastic polymers and thermosets. Additional studies[12,20–22] have shown that a plasticizing effect results when the molecules were incorporated by melt mixing in a polymer matrix; however, some studies[23,24] reported reinforcement effects in polymer-POSS nanocomposites. The occurrence of either behavior is strictly related to the chemical and/or physical interaction between POSS molecules and the matrix, and then to the structure of the inorganic cage and the organic nature of the vertex groups of the POSS molecules. Furthermore, these features are crucial factors in modulating the dispersion and in determining the morphology of a nanocomposite and its properties.

POSS molecules affect the properties in the molten state and usually act as a plasticizer; however, where strong interactions with the matrix are present, they show an anti-plasticizing effect. This last effect generally leads to higher viscosity values and improved rigidity with respect to the pristine matrix. Silanol POSS molecules are incompletely condensed silsesquioxanes containing hydroxyl groups (Si–OH) that are able to produce hydrogen bonds between their own functionalities or with different types of molecules, nanoparticles and the polar groups of the polymeric matrix.[25] Moreover, it was reported that the ability of POSS to form hydrogen bonds increases with the

[1]Dipartimento di Ingegneria Civile, Ambientale, Aerospaziale, dei Materiali, Università di Palermo, Palermo, Italy and [2]Dipartimento di Ingegneria Chimica, Gestionale, Informatica, Meccanica, Università di Palermo, Palermo, Italy
Correspondence: Professor NT Dintcheva, Dipartimento di Ingegneria Civile, Ambientale, Aerospaziale, dei Materiali, University of Palermo, Viale delle Scienze, Ed.6, Palermo 90128, Italy.
E-mail: nadka.dintcheva@unipa.it

number of Si–OH groups in the molecular structures. Roy et al.[26] studied the non-covalent interactions between POSS and sorbitol molecules because of hydrogen bonding and π–π bond interaction. However, it is not well established if these interactions can be attributed to only one of these occurrences or to their synergistic action. In melt-mixed polyoxymethylene/monosilanolisobutyl-POSS nanocomposites,[27] hydrogen bonding interactions were detected by thermal analysis. The glass temperature of nanocomposites increases with respect to that of the pristine matrix, suggesting that POSS is physically linked to the POM chains. Moreover, the low content of POSS in the nanocomposite results in antiplasticizing action.

A recent study by Toh et al.[28] on melt mixing between silanol POSS molecules and PET suggests the presence of covalent bonding between the two species at the typically high processing temperature of PET, approximately 280 °C. The silanol groups at high temperature form radicals through H extraction and so react with PET functionalities, forming stable covalent bonds between POSS molecules and the polymer matrix.

In the current study, nanocomposites based on two different polymeric matrices, ethylene-acrylic acid (EAA) copolymer and polyethylene (PE), and polyhedral oligomeric silsesquioxanes (POSS) molecules were prepared by melt mixing. The interactions between the –OH groups of POSS and the acrylic functionalities of the matrix were investigated by considering partial cage POSS with different pendent organic groups. All nanocomposites were characterized by mechanical, rheological, thermal and spectroscopic analyses. This study is a contribution to the understanding of the actions of POSS molecules in different polymer matrices. Understanding POSS behavior is very important to designing the final properties and performance of polymer-based nanocomposites.

EXPERIMENTAL PROCEDURE

The following materials were used in this study:

- Ethylene-acrylic acid (EAA) copolymer: 6% wt/wt acrylic acid, produced by Exxon-Mobil Chemical (Houston, TX, USA) under the name 'Escor 5001';
- Low-density polyethylene (PE), namely 'Riblene FC30,' produced by Polimeri Europa spa, Mantova, Italy;
- Three different polyhedral oligomeric silsesquioxane (POSS) molecules, produced by Hybrid Plastics Ltd (Hattiesburg, MS, USA): closed cage octaisobutyl POSS (IB); open cage trisilanolisobutyl POSS (TSIB) and open cage trisilanolphenyl POSS (TSPH).

The preparation of nanocomposites was accomplished using a Brabender mixer at $T = 190$ °C at a mixing speed 50 r.p.m. for 5 min. The POSS loading was 5% wt/wt, and the molecules were added to the melt after 2 min of processing. The matrices were subjected to the same processing conditions.

Rheological characterization was performed with a Rheometrics Model SR5 stress-controlled rheometer with plate-plate geometry, operating at $T = 190$ °C and 5% strain deformation. The storage modulus G' was evaluated as a function of temperature in the temperature-sweep mode using strain at 1% and frequency at 1 Hz. Mechanical tests of rectangular samples cut from compression-molded sheets (sheet thickness ∼100 μm) were carried out using an Instron (Norwood, MA, USA) materials testing machine Model 1122, according to ASTM D882 (crosshead speed of 100 mm min^{-1}). Average values of the elastic modulus (E), tensile strength (TS) and elongation at break (EB) were calculated. The reproducibility of the results was approximately ±5%.

Scanning electron microscopy (SEM) analysis was performed on nitrogen-fractured radial surfaces of the investigated samples with a Philips (Amsterdam, The Netherlands) ESEM XL30 microscope.

A Fourier transform infrared spectrometer (Spectrum One, PerkinElmer, Waltham, MA, USA) was used to record IR spectra, typically 32 scans at 1 cm^{-1} resolution in the range of 450–4000 cm^{-1}. The reported values are averages of triplicate measurements.

Calorimetric data were evaluated by differential scanning calorimetry (DSC) using a PerkinElmer DSC7 calorimeter at a scanning rate of 5 °C min^{-1}.

WAXS investigations of the neat EAA and EAA/POSS nanocomposites were carried out at room temperature in a powder Philips APD 15 diffractometer using Ni-filtered Cu Kα radiation (1.54 Å). The diffraction scans were collected between 2θ values of 10 and 30° in reflectance mode using a step of 0.05°. The obtained parameters of the individual peaks were used for further calculations: d_{hkl} spacings were calculated from the Bragg equation using the peaks corresponding to reflections along the (110) and (200) planes; the half-widths were used to determine crystallite size from the Scherer formula.

RESULTS AND DISCUSSION

Rheological analysis, consisting of viscosity measurements as a function of frequency, is very important, and the obtained results can be related to the reinforcement/plasticizing effects of the POSS molecules. In Figure 1, the viscosity curves for EAA and all EAA-based nanocomposites are reported. EAA-POSS nanocomposites show a complex viscosity higher than the values of the neat matrix over the entire investigated frequency range. However, this viscosity trend at low frequencies for EAA-TSIB is confirmed, whereas at high frequencies the viscosity values become similar to those observed for neat EAA. On the contrary, the viscosity values of PE-POSS nanocomposites are lower than the values of neat PE over the entire investigated frequency range, as shown in Figure 2.
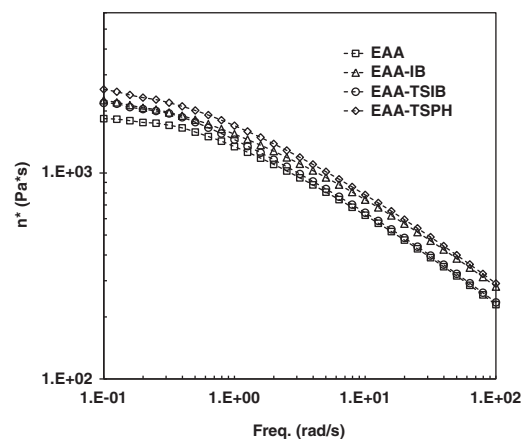

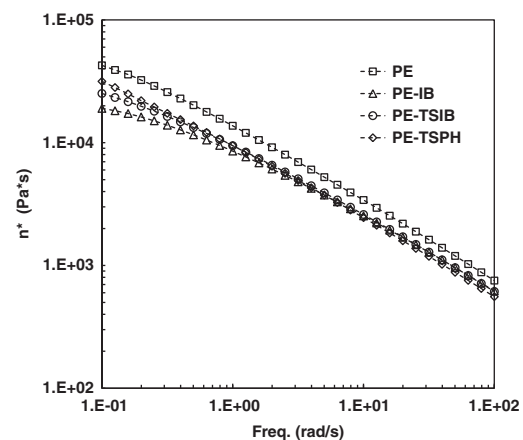**Figure 1** Viscosity curves of EAA and EAA-POSS nanocomposites.

Figure 2 Viscosity curves of PE and PE-POSS nanocomposites.

POSS molecules usually have a plasticizing role in the molten state, decreasing the matrix viscosity through an increase of the free volume, spacing the macromolecules and sometimes facilitating their slipping.[12] The rheological behavior of EAA-POSS nanocomposites seems to disagree with the well-established plasticizing action of the POSS molecules as well as that shown by PE-based nanocomposites. A possible explanation could be related to the formation of physical links because of hydrogen bonds between the –COOH groups in the matrix and the –OH groups in the POSS molecules, where present, and to the formation of POSS aggregates, which cannot be broken by the applied shear stress. The formation of chemical links between EAA and POSS is not considered because at this low processing temperature (approximately 190 °C) H extraction from the silanol groups is not favored. The conservative (G') and dissipative moduli (G'') as a function of frequency for all nanocomposites of both EAA and PE matrices confirm the observed viscosity trends but are not reported here because no additional information is added.

The trend of storage modulus as a function of temperature in dynamic temperature-sweep tests seems to confirm the formation of hydrogen interactions, as observed in Figure 3, where the G' trends for all investigated EAA-POSS nanocomposites are plotted. The storage modulus significantly decreases below 105 °C because of the melting of EAA crystals. Between 105 and 120 °C, the storage modulus shows an unexpected increase for all samples, and these trends can be related to the hydrogen bonds between –COOH matrix groups, as illustrated in the schematic representation in Figure 4a, and/or between –COOH matrix groups and the –OH groups in the POSS molecules, as illustrated in Figure 4b. Moreover, the molten state is most affected by
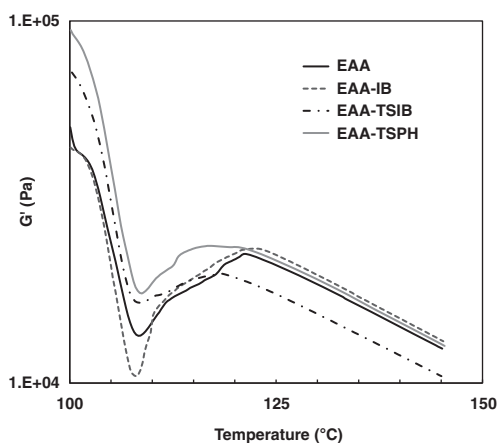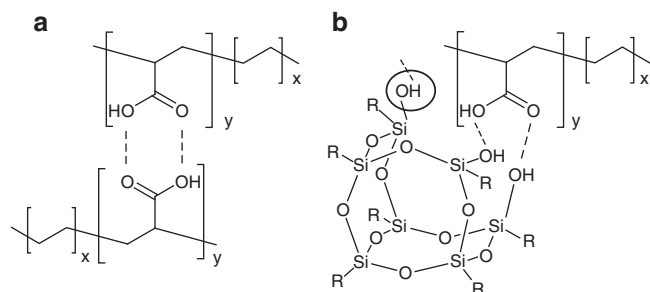
hydrogen bonds[29] because of the high availability and mobility of the macromolecules and POSS functionalities. Above ~120 °C, the G' values again decrease because hydrogen bonds are time- and temperature dependent, and, at higher temperatures, all physical interactions are destroyed. Furthermore, the G' rise for EAA-TSPH nanocomposites is more pronounced than that in pristine EAA, which may be more related to predominant physical interactions than to the plasticizing effect. The rheological behavior of EAA-TSIB nanocomposites is significantly influenced by the POSS plasticizing action and easier slipping of the macromolecules onto POSS inorganic frameworks.

The mechanical results obtained by tensile tests are reported in Table 1. Addition of IB-POSS to EAA leads to a significant increase in the elastic modulus and simultaneous significant decrease of the properties at break. These results can be understood by considering the poor compatibility between EAA and POSS molecule that aggregates and acts as a trigger for brittle fracture. The elastic modulus and tensile strength of the EAA-TSIB nanocomposite decrease, whereas the elongation at break slightly increases by ~5%; thus, this nanocomposite exhibits ductile behavior, undergoing large deformation. For the EAA-TSPH nanocomposite, the modulus increases, whereas the tensile strength and elongation at break decrease. The mechanical behavior of both EAA-TSIB and -TSPH is related to a more complex phenomenon, influenced by the filler effect, plasticizing actions and physical interactions between the macromolecules and POSS molecules that have open inorganic frameworks and contain three –OH groups.

Although the organic substituents of TSIB and TSPH have similar lengths, these two POSS molecules can show different filler effects, which is related to their affinities with the matrix and to the conformational structures of the organic pendent groups. In particular, the IB pendent groups can roll up and form some entanglements, while the PH-rings are rigid structures with stable conformations. Thus, the IB groups and PH-rings have similar lengths, but the TSIB- and TSPH-POSS molecules in the nanocomposite occupy different volume fractions because the conformations of the IB groups and PH-rings are different; consequently, these two POSS molecules exert different filler effects. Therefore, in the solid state, the plasticizing effect of the TSIB molecules is predominant rather than the effect of the physical interactions, while the TSPH molecules act as an antiplasticizer.

However, in PE-based nanocomposites, where hydrogen bonds between macromolecules and POSS molecules cannot occur because functionalities are not present, the plasticizing effect is evident, although in the solid state, this plasticizing effect is less pronounced

Figure 3 Modulus G' of EAA and EAA-POSS nanocomposites with respect to temperature.

Figure 4 Schematic interpretation of hydrogen bonds in (**a**) EAA dimers and (**b**) EAA-silanol POSS nanocomposites.

Table 1 Mechanical (elastic modulus, E, tensile strength, TS and elongation at break, EB) and thermal (melting temperature, Tm and fusion enthalpies, ΔH, of first heating) properties for neat matrices and nanocomposites

Sample	E (Mpa)	TS (MPa)	EB (%)	T_m (°C)	ΔH (J g^{-1})
EAA	103	17.5	360	99.1	47.9
EAA-IB	129	11.7	135	98.0	46.4
EAA-TSIB	95	11.8	380	96.5	41.4
EAA-TSPH	132	14.7	270	98.4	42.8
PE	135	15.5	530	107.4	62.7
PE-IB	142	5.5	100	107.4	61.1
PE-TSIB	138	12.0	598	106.8	51.7
PE-TSPH	147	12.5	550	107.3	59.3

than in the molten state. Particularly, the elastic moduli of TSIB- and TSPH-based nanocomposites remain almost unchanged, whereas elongation at break slightly increases. However, the IB-based nanocomposite shows brittle mechanical behavior (elongation at break is five times lower than that of neat PE), which can be due to the formation of aggregates.

In Figures 5 and 6, the thermogram curves of the second heating scans are shown, and, in the last two columns of Table 1, the fusion temperatures and enthalpies of all investigated samples are reported. The variations of the fusion temperature of both EAA and PE matrices upon POSS addition are almost negligible, whereas the variations of the fusion enthalpies are influenced by the POSS varieties and possible interaction between the matrices and POSS molecules. Moreover, IB-EAA and IB-PE nanocomposites show similar fusion enthalpy decreases, ~3%, relative to those of the neat EAA and PE matrices. The IB molecules show a tendency to aggregate because of their limited dispersion into the polymers, as discussed in the morphology section below. Upon IB addition, both EAA and PE matrices lose their ductility, as discussed above. TSIB molecules significantly decrease the fusion enthalpies for both matrices, and these reductions are ~16% that of neat EAA and PE. The drastic decrease of the fusion enthalpies without loss in ductility suggests a rather distinct plasticizing effect of this type of POSS molecule.
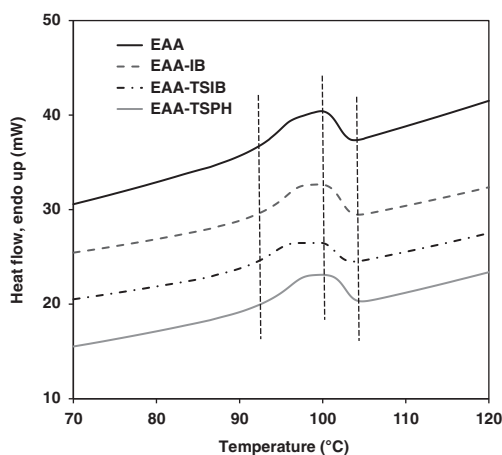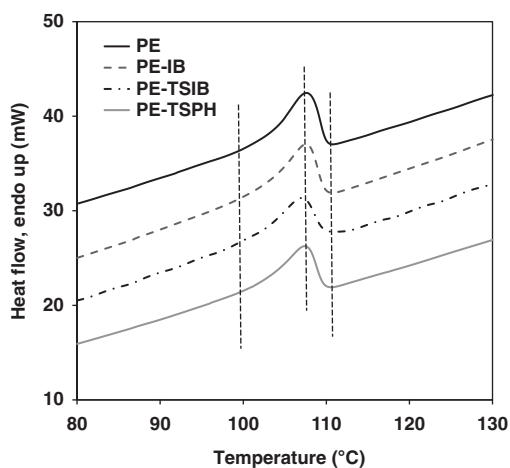
Although TSIB molecules can interact with the acrylic functionalities through hydrogen bonds, their ability to facilitate the slipping of the macromolecules is a predominant phenomenon, and their overall action is plasticization, which is also due to the flexibility of the open inorganic frameworks and short pendent organic groups, as widely investigated in our previous study.[10] Furthermore, the addition of TSPH molecules leads to a decrease in the fusion enthalpies for both matrices, even if their action must be evaluated by considering the type of matrix. The EAA-TSPH sample shows a pronounced reduction in fusion enthalpies, ~10% relative to that of the neat matrix, whereas this diminution for PE-TSPH samples is only ~5% with respect to neat PE.

As demonstrated in the literature,[26] the crystalline zones in neat EAA are formed only by macromolecular segments, where the functionalities are not present, as in the [x] segment in Figure 4a. In this way, the acrylic functionalities that surrounded the crystalline zones of EAA are available to interact with the –OH groups in the silanol POSS molecules. Because of the interaction between the TSPH molecules and EAA macromolecules, the crystalline zones are less perfect than the neat matrix, and total fusion enthalpy decreases. For the PE matrix, TSPH molecules are able to act only as a plasticizer, increasing the free volume and spacing the macromolecules; for this reason, the reduction in fusion enthalpy is not drastic.

To elucidate the thermal behavior of EAA-based nanocomposites, X-ray diffraction analysis of neat EAA and EAA-POSS nanocomposites was performed. The X-ray diffraction patterns are reported in Figure 7. For neat EAA, the most intense diffraction peaks are observed at $2\theta = 21.35$ and 23.70°, corresponding to reflections along the (110) and (200) crystallographic planes, respectively, of the orthorhombic crystal lattice of the polyethylene fraction in EAA, as documented in the literature.[30] The addition of POSS does not significantly modify the position of the diffraction peaks of the EAA matrix. In Table 2, the calculated lattice spacing (d_{hkl}) and crystalline size (L_{110}) along the (110) crystallographic planes of the orthorhombic EAA crystal lattice are listed. These dimensions are clearly smaller in EAA-TSIB and -TSPH nanocomposites than in neat EAA and EAA-IB samples. These results could be interpreted as a disturbance of the crystallization of PE segments bonded with acrylic acid due to the H-interaction with–OH in the POSS silanols.

Figure 5 Thermograms of EAA and EAA-POSS nanocomposites.

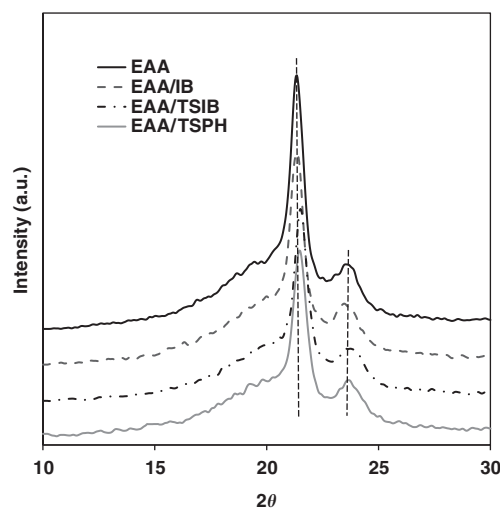Figure 6 Thermograms of PE and PE-POSS nanocomposites.

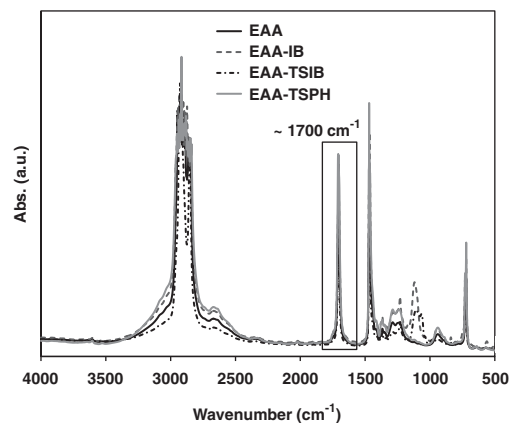Figure 7 X-ray diffraction patterns of neat EAA and EAA-POSS nanocomposites.

Moreover, to better understand the behavior in the solid state, we must consider the morphology achieved on addition of POSS and the physical interactions between POSS molecules and macromolecules with functionalities. The EAA-POSS system morphology is observed by SEM analysis (Figure 8). The formation of POSS aggregates at the microscopic level on the fractured surface of an EAA-IB sample is clearly observed, as confirmed by the EDX-SEM analysis shown in the insert in Figure 8b; dimensions of the IB-POSS aggregates are ~ 10 μm. Furthermore, the TSIB- and TSPH-POSS in the EAA matrix at this magnification show better dispersion and distribution, and micrometric aggregates are not observed. In particular, small TSIB aggregates (Figure 8c) are covered by the EAA macromolecules, and no clear separation from the matrix can be observed.

The physical interactions between the macromolecules with functionalities and POSS molecules were investigated by FT-IR spectroscopy (Figure 9). The presence of the characteristic peaks for all investigated EAA-based samples at $\sim 1700\,cm^{-1}$ (indicated zone in Figure 9) is due to the formation of physical interactions between the polar acrylic groups preset in the structure of EAA sample, which is well-known from the literature.[26] The FT-IR spectra of PE-based nanocomposites are not reported here because the lack of functionalities in the structure of PE results in no characteristic peak formation at $\sim 1700\,cm^{-1}$. The accurate analysis of the FT-IR spectra in the specific wave number range between 1750 and $1650\,cm^{-1}$ of EAA samples shows a quite distinct peak at $1705\,cm^{-1}$ (Figure 10) that is related to dimers caused by hydrogen bonding between fractions of acrylic acid. In addition, a secondary peak at $1700\,cm^{-1}$ and a small shoulder at $\sim 1698\,cm^{-1}$ are also related to the presence of non-conjugated acrylic functionalities.

Figure 9 FT-IR spectra of EAA and EAA-POSS nanocomposites.

Table 2 Lattice spacing, d and crystalline size, L, of the EAA and EAA-POSS samples

Sample	d_{110} (Å)	d_{200} (Å)	L_{110} (Å)
EAA	4.16	3.75	302
EAA-IB	4.16	3.78	302
EAA-TSIB	4.12	3.74	290
EAA-TSPH	4.13	3.76	255
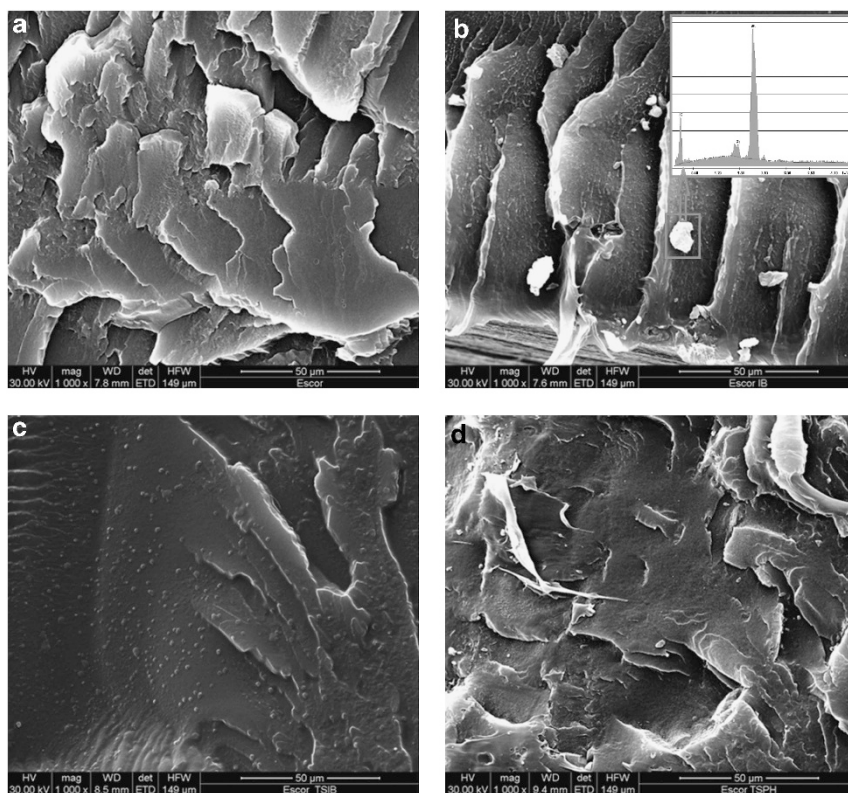
Figure 8 SEM micrographs of (**a**) EAA and EAA-POSS nanocomposites, particularly (**b**) EAA-IB, (**c**) EAA-TSIB, (**d**) EAA-TSPH. A full color version of this figure is available at *Polymer Journal* online.
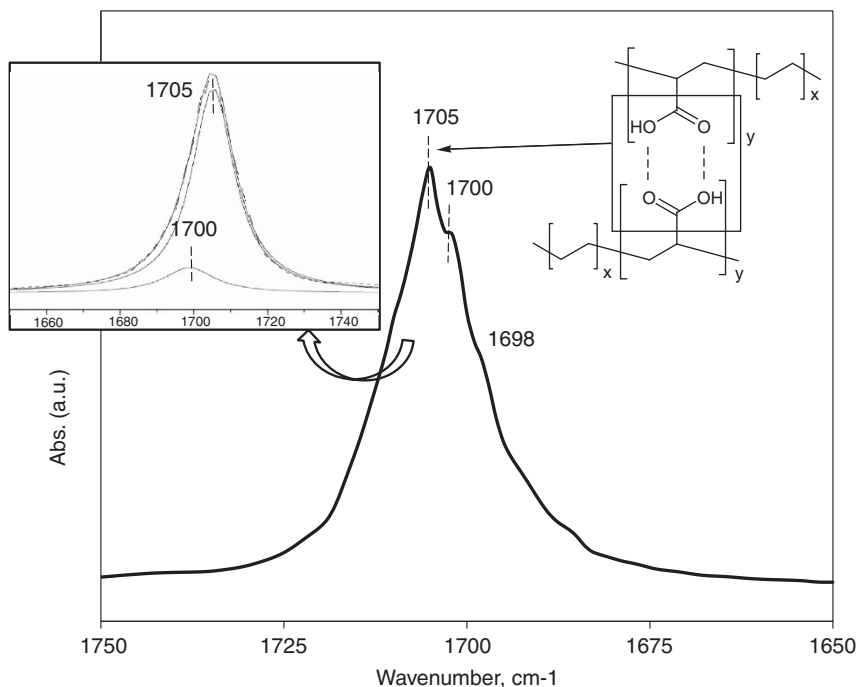
Figure 10 FT-IR spectra in the range 1750–1650 cm^{-1} of EAA sample; the inset shows peak deconvolution.
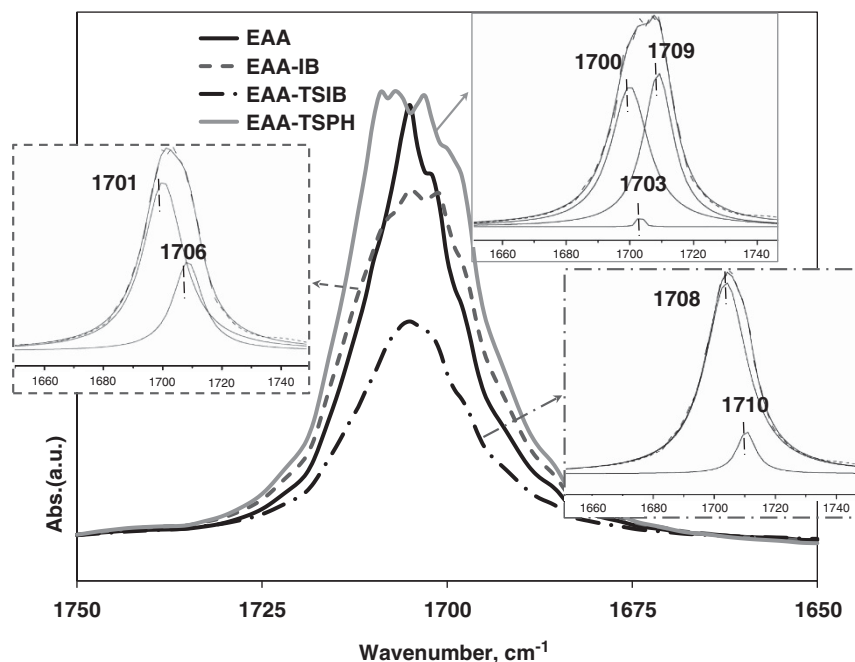

Figure 11 FT-IR spectra in the range 1750–1650 cm^{-1} of EAA-POSS nanocomposites; insets show peak deconvolution.

The deconvolution of the peaks between 1650 and 1750 cm^{-1}, shown in the inset in Figure 10, confirms that the interactions in the EAA structure are mainly due to the formation of dimers between acrylic functionalities, estimated as the ratio of the areas of the deconvoluted peaks ($A_{1705cm^{-1}}/A_{1700cm^{-1}}$). The wave number scale of the inset figure is in inverse order; the dashed line is the FT-IR spectra (experimental curve), whereas the continuous line is the fitting curve of the deconvoluted peaks. The overlap between these two curves

suggests the goodness of the spectra deconvolution. The FT-IR spectrum of an EAA-IB sample is similar to that of the pristine matrix; the shift of both peaks is negligible, even if the height of the main peak (~ 1705 cm^{-1}) is lower than the EAA peak (Figure 11).

Notably, the deconvolution of peaks suggests the reduced presence of dimers for the EAA-IB sample relative to the neat matrix; the ratio of the areas of the deconvoluted peaks ($A_{1706cm^{-1}}/A_{1701cm^{-1}}$) is reversed from the ratio for neat EAA. EAA-TSIB shows a

significantly lower peak at ~1708 cm^{-1}, and, as noticeable from the peak deconvolution, two peaks are visible, at exactly 1708 and 1710 cm^{-1}. The deconvolution of the spectra for the TSPH-EAA sample shows the presence of different peaks at 1709, 1703 and 1700 cm^{-1}. The shift of the peaks toward higher wave numbers and the peak splitting suggests the occurrence of physical interactions, different from those of the EAA dimers, between the acrylic functionalities and –OH groups of POSS cages, confirming the formation of hydrogen bonds.

CONCLUSIONS

POSS molecules with different functionalities may assume different functions for the polymer matrix, depending on their potential interactions. Particularly, in this study, the physical interactions between POSS molecules with –OH functionalities and an EAA matrix with acrylic functionalities were studied. Furthermore, the impact of these interactions on the properties in molten and solid states was accurately investigated. PE-POSS nanocomposites were prepared under the same processing conditions for sake of comparison. All nanocomposites were characterized by mechanical, rheological and spectroscopic analyses. The EAA-POSS nanocomposites showed peculiar rheological behavior that can be understood by considering the formation of a physical network due to hydrogen bonds between –COOH groups in the matrix and –OH groups in the POSS molecules. The mechanical results obtained by tensile tests confirm the antiplasticizing effect of the POSS for systems in which interactions between macromolecules and POSS molecules are present. However, the inorganic framework of POSS exerts a plasticizing effect, and all measured properties are results of two contrasting phenomena, the plasticizing and reinforcement effects.

1 Provatas, A. & Matisons, J. G. Silsesquioxanes: synthesis and applications. *Trends Polym. Sci.* **5**, 327–332 (1997).
2 Kuo, S.-W. & Chang, F.-C. POSS related polymer nanocomposites. *Progress Polym. Sci.* **36**, 1649–1696 (2011).
3 Gnanasekaran, D., Madhavpan, K. & Reddy, R. S. R. Developments of polyhedral oligomeric silsesquioxanes (POSS), POSS nanocomposites and their applications: a review. *J. Sci. Ind. Res.* **68**, 437–464 (2009).
4 Misra, R., Alidedeoglu, A. H., Jarrett, W. L. & Morgan, S. E. Molecular miscibility and chain dynamics in POSS/polystyrene blends: control of POSS preferential dispersion states. *Polymer (Guildf).* **50**, 2906–2918 (2009).
5 Zhang, W., Fang, B., Walther, A. & Müller, A. Synthesis via RAFT polymerization of Tadpole-shaped Organic/inorganic hybrid PAA containing POSS and their self-assembly in water. *Macromolecules* **42**, 2563–2569 (2009).
6 Mori, H., Sada, C., Konno, T. & Yonetakea, K. Synthesis and characterization of low-refractive-index fluorinated silsesquioxane-based hybrids. *Polymer (Guildf)* **52**, 5452–2463 (2011).
7 Dintcheva, N. T. z., Morici, E., Arrigo, R., La Mantia, F. P., Malatesta, V. & Schwab, J. J. UV-stabilisation of polystyrene-based nanocomposites provided by polyhedral oligomeric silsesquioxanes (POSS). *Polym. Degrad. Stab.* **97**, 2313–2322 (2012).
8 Zhao, H., Shu, J., Chen, Q. & Zhang, S. Quantitative structural characterization of POSS and octavinyl-POSS nanocomposites by solid state NMR. *Solid State Nucl. Mag.* **43**, 56–61 (2012).
9 Markovic, E., Matisons, J., Hussain, M. & Simon, G. P. Poly(ethylene glycol) octafunctionalized polyhedral oligomeric silsesquioxane: WAXD and rheological studies. *Macromolecules* **40**, 4530–4534 (2007).
10 Chang, Y. W. & Shin, G. Crosslinked poly(ethylene glycol) (PEG)/sulfonated polyhedral oligosilsesquioxane (sPOSS) hybrid membranes for direct methanol fuel cell applications. *J. Ind. Eng. Chem.* **17**, 730–735 (2011).
11 Song, M. M., Duo, S. W. & Liu, T. Z. Effects of atomic oxygen irradiation on PDMS/POSS hybrid films in low earth orbit environment. *Adv. Mat. Res.* **239**, 1368–1371 (2011).
12 Dintcheva, N. T. z., Morici, E., Arrigo, R., La Mantia, F. P., Malatesta, V. & Schwab, J. J. Structure-properties relationships of polyhedral oligomeric silsesquioxane (POSS) filled PS nanocomposites. *Express Polym. Lett.* **6**, 561–571 (2012).
13 Lu, C. H., Wang, J. H., Chang, F. C. & Kuo, S. W. Star block copolymers through nitroxide-mediated radical polymerization from polyhedral oligomeric silsesquioxane (POSS) Core. *Macromol. Chem. Phys.* **211**, 1339–1347 (2010).
14 Fu, B. X., Gelfer, M. Y., Hsiao, B. S., Phillips, S., Viers, B., Blanski, R. & Ruth, P. Physical gelation in ethylene–propylene copolymer melts induced by polyhedral oligomeric silsesquioxane (POSS) molecules. *Polymer (Guildf)* **44**, 1490–1506 (2003).
15 Engstrand, J., López, A., Engqvist, H. & Persson, C. Polyhedral oligomeric silsesquioxane (POSS)–poly(ethylene glycol) (PEG) hybrids as injectable biomaterials. *Biomed. Mater.* **7**, 035013–035022 (2012).
16 DeArmitt, C. & Wheeler, P. POSS keeps high temperature plastics flowing. *Plast. Addit. Comp.* **10**, 36–39 (2008).
17 Fina, A., Tabuani, D. & Camino, G. Polypropylene–polysilsesquioxane blends. *Eur. Polym. J.* **46**, 14–23 (2010).
18 Tang, Y. & Lewin, M. Migration and surface modification in polypropylene (PP)/polyhedral oligomeric silsesquioxane (POSS) nanocomposites. *Polym. Advan. Technol.* **20**, 1–15 (2009).
19 Fina, A., Bocchini, S. & Camino, G. Catalytic fire retardant nanocomposites. *Polym. Degrad. Stab.* **93**, 1647–1655 (2008).
20 Wu, J., Haddad, T. S. & Mather, P. T. Vertex group effects in entangled polystyrene-polyhedral oligosilsesquioxane (POSS) copolymers. *Macromolecules* **42**, 1142–1152 (2009).
21 Soong, S. Y., Cohen, R. E. & Boyce, M. C. Polyhedral oligomeric silsesquioxane as a novel plasticizer for poly(vinyl chloride). *Polymer (Guildf)* **48**, 1410–1418 (2007).
22 Zhang, X., Sun, J., Wang, C., Jia, T., Li, Y. & Fang, S. Substituents effects on the properties of polyhedral oligomeric silsesquioxanes(POSS)/poly(L-lactic acid) hybrid films. *J. Macromol. Sci. Pure. Appl. Chem.* **49**, 73–80 (2012).
23 Iyer, S. & Schiraldi, D. A. Role of specific interactions and solubility in the reinforcement of bisphenol A polymers with polyhedral oligomeric silsesquioxanes. *Macromolecules* **40**, 4942–4952 (2007).
24 Durmus, A., Kasgoz, A., Ercan, N., Akn, D. & Şanl, S. Effect of polyhedral oligomeric silsesquioxane (POSS) reinforced polypropylene (PP) nanocomposite on the micro-structure and isothermal crystallization kinetics of polyoxymethylene (POM). *Polymer (Guildf)* **53**, 5347–5357 (2012).
25 Liu, H., Kondo, S., Tanaka, R., Oku, H. & Unno, M. A spectroscopic investigation of incompletely condensed polyhedral oligomeric silsesquioxanes (POSS-mono-ol, POSS-diol and POSS-triol): Hydrogen-bonded interaction and host–guest complex. *J. Organomet. Chem.* **693**, 1301–1308 (2008).
26 Roy, S., Scionti, V., Jana, S. C., Wesdemiotis, C., Pischera, A. M. & Espe, M. P. Sorbitol–POSS interactions on development of isotactic polypropylene composites. *Macromolecules* **44**, 8064–8079 (2011).
27 Illescas, S., Sánchez-Soto, M., Milliman, H., Schiraldi, D. A. & Arostegui, A. The morphology and properties of melt-mixed polyoxymethylene/monosilanolisobutyl-POSS composites. *High Perform. Polymer.* **23**, 457–467 (2011).
28 Toh, C. H. L., Yang, L., Pramoda, K. P., Lau, S. K. & Lu, X. Poly(ethylene terephthalate)/clay nanocomposites with trisilanolphenyl polyhedral oligomeric silsesquioxane as dispersant: simultaneously enhanced reinforcing and stabilizing effects. *Polym. Int.* **62**, 1492–1499 (2013).
29 Otocka, E. P. & Kwei, T. K. Properties of ethylene-acrylic acid copolymers. *Macromolecules* **1**, 244–249 (1968).
30 Minkova, L. & Magagnini, P. Characterization of a PE-g-LCP compatibilizer, prepared by reactive blending of acrylic acid grafted polyethylene (PE) and a semiflexible liquid crystalline polymer (LCP). *Macromol. Chem. Phys.* **200**, 2551–2558 (1999).